Molecular Crystals and Liquid Crystals Science and Technology. Section A. Molecular Crystals and Liquid Crystals
Publication details, including instructions for authors and subscription information:
http://www.tandfonline.com/loi/gmcl19

Z-Scan Measurements on Liquid Crystals: Some Considerations and Results

P. Palffy-muhoray [a], T. Wei [a] & W. Zhao [a]
[a] Liquid Crystal Institute and Department of Physics, Kent State University, Kent, Ohio, 44242, U.S.A.
Version of record first published: 24 Sep 2006.

To cite this article: P. Palffy-muhoray , T. Wei & W. Zhao (1994): Z-Scan Measurements on Liquid Crystals: Some Considerations and Results, Molecular Crystals and Liquid Crystals Science and Technology. Section A. Molecular Crystals and Liquid Crystals, 251:1, 19-31

To link to this article: http://dx.doi.org/10.1080/10587259408027189

Mol. Cryst. Liq. Cryst. 1994, Vol. 251, pp. 19–31
Reprints available directly from the publisher
Photocopying permitted by license only

Printed in the United States of America

Z-SCAN MEASUREMENTS ON LIQUID CRYSTALS: SOME CONSIDERATIONS AND RESULTS

P. PALFFY-MUHORAY, T. WEI and W. ZHAO
Liquid Crystal Institute and Department of Physics, Kent State University, Kent, Ohio 44242, U.S.A.

Abstract Using the Z-scan technique, we study the intensity dependent response of liquid crystals in geometries where director reorientation is not expected. The dependence of Z-scan results on spatial beam profile is examined by comparison of results obtained from Gaussian and top-hat beams. Effects of response times on the measured nonlinearities are also discussed. Physical mechanisms for the observed optical nonlinearities on the nanosecond timescale are proposed.

Nematic liquid crystals possess some of the highest known optical nonlinearities. Due to inversion symmetry, the first nonvanishing nonlinear term is of third-order. It can be described by the nonlinear polarization

$$\mathbf{P}^{(3)}(\omega) = \chi^{(3)}(\omega;\omega,-\omega,\omega)\mathbf{E}\mathbf{E}^*\mathbf{E}, \tag{1}$$

where $\chi^{(3)}$ is the third-order susceptibility, whose real and imaginary parts are related to the nonlinear refractive index n_2 and absorption coefficient β, by

$$\mathrm{Re}\chi^{(3)} = 2n_0 n_2, \tag{2}$$

$$\mathrm{Im}\chi^{(3)} = \frac{\lambda n_0^2 \epsilon_0 c}{2\pi}\beta. \tag{3}$$

n_2 and β are the intensity-dependent contributions to the refractive index n and the absorption coefficient α

$$n = n_0 + \frac{n_2}{2}E^2 = n_0 + \gamma I, \tag{4}$$

$$\alpha = \alpha_0 + \beta I, \tag{5}$$

where I is the incident intensity, n_0 is the linear refractive index and α_0 is the linear absorption coefficient.

Two practical methods to measure the intensity-dependent nonlinearities of liquid crystals are the degenerate four-wave mixing (DFWM) and the Z-scan method. The former measures the intensity of the signal diffracted by the grating created in the liquid crystal. As a result, the signal intensity is proportional to the square of the induced polarization,

$$I_{out} \sim (P^{(3)})^2 \sim (\chi^{(3)})^2 I_{in}^3. \tag{6}$$

While a sensitive method, DFWM cannot be used to determine the sign of $\chi^{(3)}$. The Z-scan method, on the other hand, is based on self-focusing and defocusing, where the measured signal is,

$$I_{out} \sim (\epsilon_0 E_{in} + P^{(3)})^2 \sim I_{in} + 2\chi^{(3)} I_{in}^2 + \ldots. \tag{7}$$

Thus, the measured signal is linear in $\chi^{(3)}$, and can be used to determine both the sign and the magnitude of $\chi^{(3)}$. In an addition, the Z-scan technique uses a single beam, which simplifies the experiment.

The Z-scan technique was developed by the research group in CREOL.[1,2] The method consists of moving the sample along the axis of a focused beam, and measuring the transmitted intensity with a detector behind an aperture. The intensity dependent nonlinearities cause the measured intensity to vary with sample position, and analysis of the data, obtained with and without the aperture, allows the determination of the signs and magnitudes of the nonlinear index n_2 and the nonlinear absorption coefficient β. A schematic of the experimental setup is shown in Fig. 1. Typical experimental results are also shown there.

For Gaussian beams, the Z-scan curves (transmittance as a function of sample position z) have the form[3]

$$T_N = 1 - \frac{4x}{(1+x^2)(9+x^2)} \frac{2\pi\gamma I_0 L}{\lambda} - \frac{1}{1+x^2} \frac{\beta I_0 L}{2\sqrt{2}}, \tag{8}$$

for small aperture ($A \leq 0.1$) and

$$T_N = 1 - \frac{1}{1+x^2} \frac{\beta I_0 L}{2\sqrt{2}}, \tag{9}$$

without the aperture ($A = 1$). Here $x = z/z_0$ is the normalized sample position, z_0 is the Rayleigh range, A is the aperture transmittance, L is the sample thickness, I_0 is the on-axis intensity of the incident beam, and λ is the wavelength.

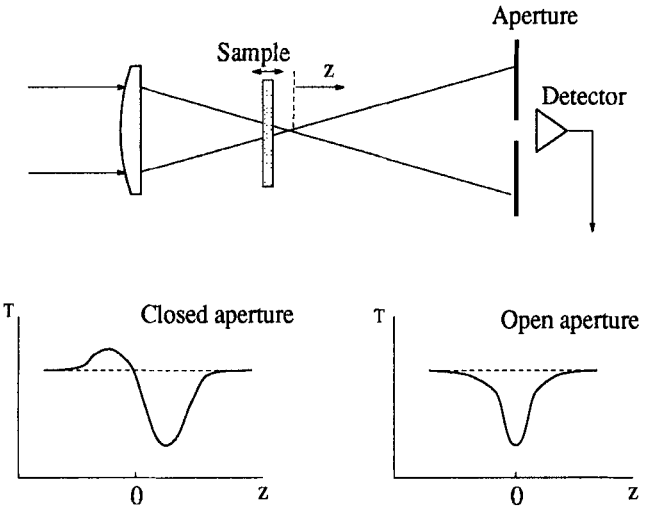

Figure 1: Experimental setup and typical measured data for Z-scan measurements.

We have carried out Z-scan measurements of β and n_2 for liquid crystals on milli-, nano-, and pico-second time scales using Gaussian beams. Fig. 2 shows the spatial and temporal profiles of the picosecond pulses used in the Z-scan measurements. Fig. 3 shows the Z-scan curves obtained with ps pulses for CS_2, which was used to verify calibration. The uncertainty in the measurement is less than 5%. The data of Z-scan measurements are given in Fig. 4.

The conventional Z-scan technique is predicated on using Gaussian beams. Since Gaussian beam profiles are not always readily available, as in the case of most dye lasers, we have developed and tested a method of determining n_2 and β from Z-scan data using top-hat rather than Gaussian beams. This opens the door to the determination of the wavelength dependence of the third order response. A good approximation to the top-hat profile can be obtained by truncating a large diameter collimated beam by a small aperture.

The analysis of the Z-scan data using top-hat beams begins with the beam propagation from the entrance aperture to the sample, which can be written as a superposition of Lommel functions.[4] The nonlinear phase shift and absorption caused by the sample are accounted for by the real and imaginary phase shift of the incident beam, ignoring the variation of the beam due to propagation in the sample, which is valid for thin samples. The field distribution in the far field can

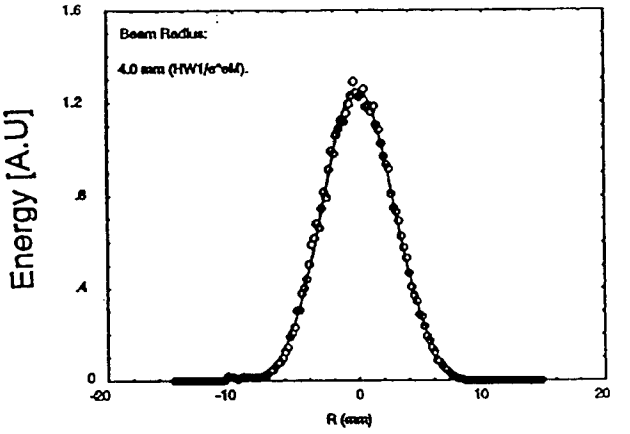

(a)

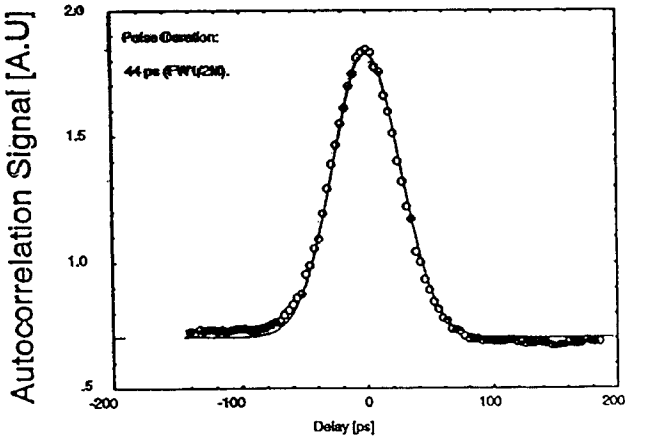

(b)

Figure 2: The spatial profile (a) and the autocorrelation (b) of the pulses generated from a mode-locked and frequency-doubled Nd:YAG laser.

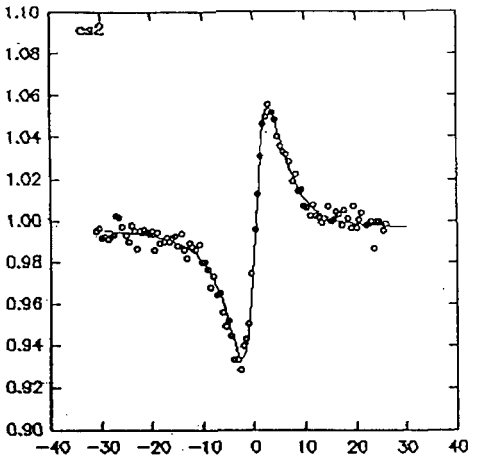

Figure 3: Z-scan measurement of n_2 for CS_2. Numerical fitting was done using $n_2 = 1.25 \times 10^{-11}$.

be obtained from the Fourier transform of that at the exit surface. Instead of doing the analysis point by point, we have carried out a general calculation for both β and n_2. β and n_2 can be obtained from experimental measurements via the the chart, shown in Fig. 5.

To use the chart, the imaginary phase shift (the coefficient of nonlinear absorption) Ψ, is first determined from the measured T_{pv}^1 using the left hand portion of the chart. From this value of Ψ and from the measured T_{pv}^0, the real phase shift Φ_0 (the nonlinear phase shift), can be obtained from the right hand portion of the chart. After these two are determined, β and n_2 are given by:

$$\beta = \frac{\Psi}{L_{eff} I_0}; \qquad \text{and} \qquad \gamma = \frac{\Phi_0 \lambda}{2\pi L_{eff} I_0}. \tag{10}$$

Z-scan results using top-hat beams are verified[5] with a CS_2 sample using laser pulses from a dye laser at a wavelength $\lambda = 563$ nm, pumped by a Q-switched and frequency doubled Nd:YAG laser, shown in Fig. 6.

The results for β and n_2 are shown in Fig. 7.

We note that the magnitudes of the optical nonlinearities vary over many orders of magnitude on the time scales ranging from milli- to picosecond. To explore this phenomenon, we have studied the response times of the underlying physical process. For laser pulses with duration τ_L, the measured nonlinearity $\chi^{(3)}_{meas}$ is the

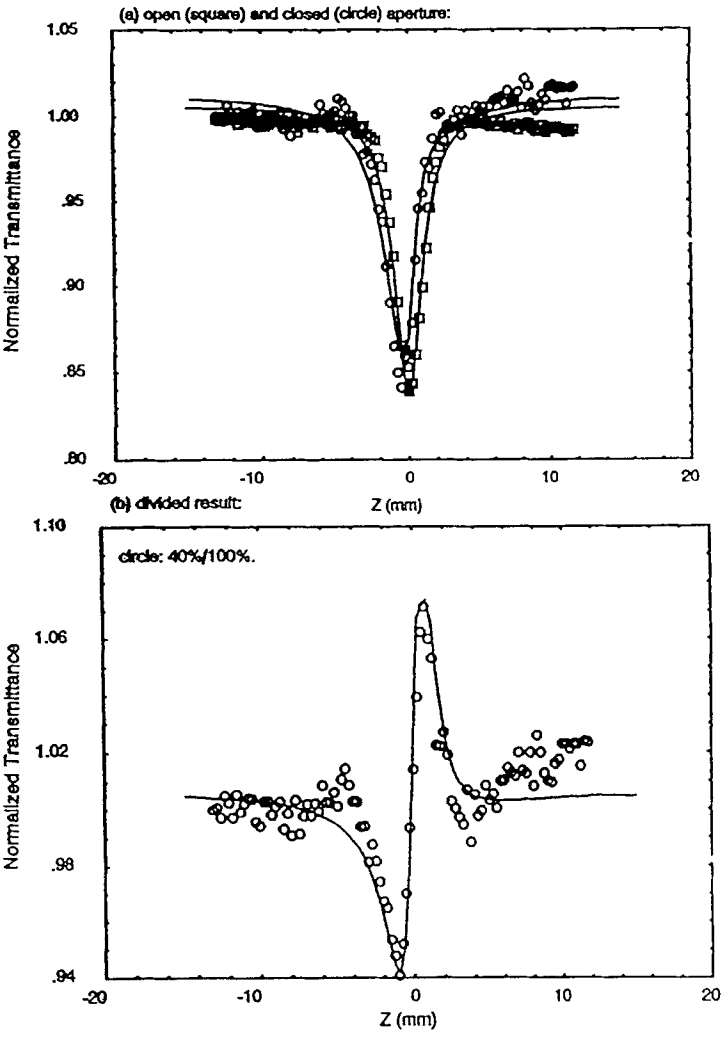

Figure 4: Z-scan curves obtained with the ps pulses for 8CB at a wavelength of $\lambda = 532$nm. The energy of the incident pulse is 1.3 μJ. Theoretical fitting was obtained with $\beta = 4$ cm/GW and $n_2 = 7.6 \times 10^{-12}$ esu.

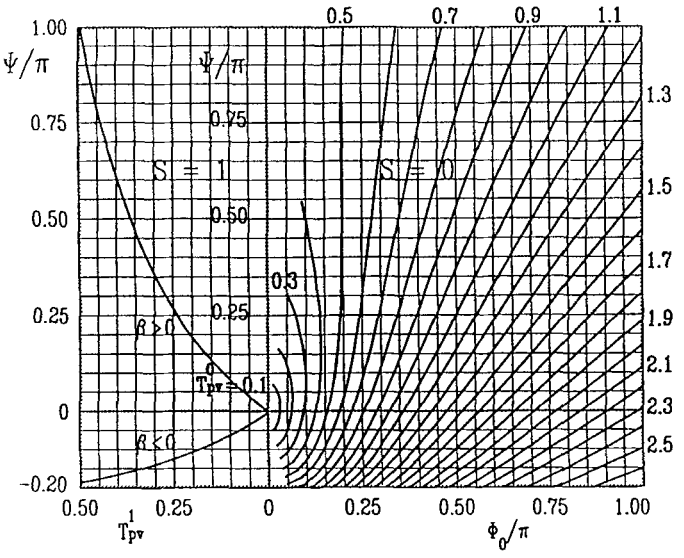

Figure 5: T_{pv}^{1} is the measured peak-valley difference without aperture ($S = 1$), $T_{pv}0$ measured peak-valley difference with a small aperture, $\Psi = \beta I_0 L_{eff}$ the imaginary phase shift caused nonlinear absorption, $\Phi_0 = 2\pi\gamma I_0 L/\lambda$, and $L_{eff} = (1 - e^{-\alpha L})/\alpha$.

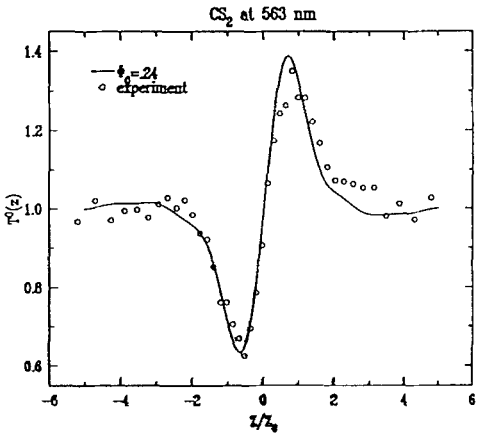

Figure 6: Experimental result of Z-scan measurements of $\chi^{(3)}$ for CS_2 using top-hat beams.

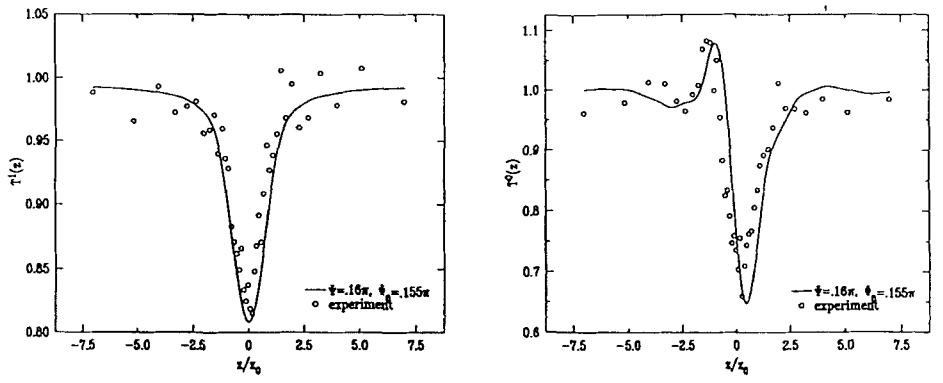

Figure 7: Experimental result of Z-scan measurements of $\chi^{(3)}$ using top-hat beams. The sample is a nematic 5CB, with its director parallel to the polarization of the incident beam.

time average of the nonlinear response over the pulse duration,

$$\chi^{(3)}_{meas} = < \chi^{(3)} > \tau_L = \frac{1}{\tau_L < I_0 >} \int \int \chi^{(3)}(t - t') I_0(t') dt dt'. \tag{11}$$

If the process has a single response time τ,

$$\chi^{(3)}_{meas} = \frac{\chi^{(3)}}{1 + \frac{\tau}{\tau_L}} = \begin{cases} \chi^{(3)} & \text{for } \tau \ll \tau_L \\ \frac{\tau_L}{\tau} \chi^{(3)} & \text{for } \tau \gg \tau_L \end{cases} \tag{12}$$

Therefore the contribution of slow processes decreases with shorter pulses.

The liquid crystal samples are typically prepared using glass cells spin-coated with a polyimide layer, which is buffed to produce planar alignment. The liquid crystal is sandwiched between two glass plates, spaced typically at 25 μm. The incident beam is polarized either parallel or perpendicular to the nematic director. In such a configuration, no director reorientation is expected to occur. The measured values then corresponds to the real and imaginary parts of $\chi^{(3)}_{3333}$ and $\chi^{(3)}_{1111}$, respectively. When the temperature of the sample is above the nematic-isotropic transition temperature, the measurement is independent of polarization of the incident beam and the measurement gives $\chi^{(3)}$ in the isotropic phase.

The results for 5CB are, on different time scales,[6]

τ_L	λ	$n_{2\|\|}$ (esu)	$n_{2\perp}$ (esu)	n_{2i}	$\beta_{\|\|}$ cm/GW	$\beta_\perp$	β_i
10 ms	514 nm	-10×10^{-4}	$+2 \times 10^{-4}$	-2×10^{-4}	0	0	0
7 ns	532 nm	-5×10^{-10}	$+1 \times 10^{-10}$	-2×10^{-10}	265	36	114
30 ps	532 nm	$+10 \times 10^{-12}$	$+6 \times 10^{-12}$	NA	2.2	0.8	NA

As can be seen above, dramaticly different values of $\chi^{(3)}$ are obtained with laser pulses of different duration. Different mechanisms may therefore be responsible for the nonlinearities on different time scales.

On the millisecond time scale, laser heating due to linear absorption causes the refractive index to change with incident intensity. This is evidenced by the temperature dependence of the measured $\chi^{(3)}$. Due to laser heating, both the order parameter S and density ρ decrease. The refractive indices change according to the relations:

$$n_{||} = n_i + \rho \Delta S, \tag{13}$$

$$n_\perp = n_i - \frac{1}{2}\rho \Delta S. \tag{14}$$

When the temperature approaches the nematic-isotropic transition, the order parameter diverges, as shown in Fig. 8.

On the nanosecond time scale, the values of $\chi^{(3)}$ remain almost independent of temperature within the nematic range of 5CB. The measured value of $\chi^{(3)}$ is determined by two processes: thermal diffusion with time constant τ_D and order parameter relaxation with a time constant τ_S. For a 6 ns pulse, where $\tau_D/\tau_L > 1$ and $\tau_S/\tau_L > 1$, the experimentally measured $\chi^{(3)}$ from the Z-scan measurement is

$$\chi^{(3)}_{meas} = \frac{\chi^{(3)}}{(1+\frac{\tau_D}{\tau_L})(1+\frac{\tau_S}{\tau_L})} \simeq \frac{\tau_L^2}{\tau_D \tau_S}\chi^{(3)}. \tag{15}$$

Near T_{NI}, $\chi^{(3)} \sim (T - T_{NI})^{-1/2}$ and $\tau_S \sim (T - T_{NI})^{-1/2}$,[7] and the temperature dependence of the measured $\chi^{(3)}$ is cancelled for nanosecond pulses, resulting in the observed temperature independence of $\chi^{(3)}$ for 5CB.

We studied time response of the optical nonlinearities of $\chi^{(3)}$ using a 2-pulse Z-scan scheme. Two pulses, each having a 6 ns pulse duration but separated from each other by 10 ns, are used in the Z-scan measurement.[8] If the response of the

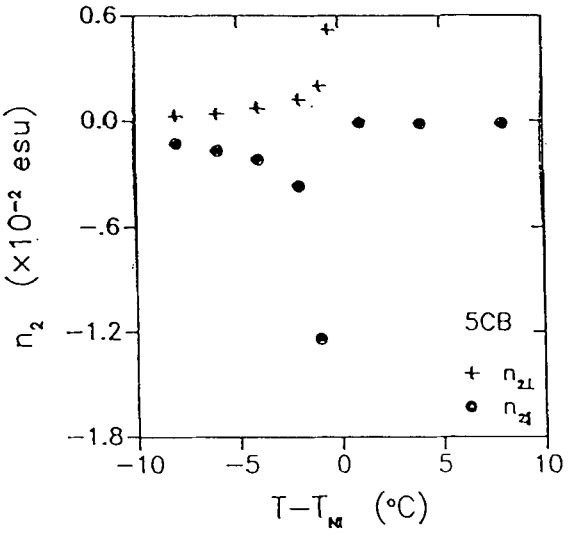

Figure 8: The temperature dependence of the nonlinear birefringence of 5CB measured with millisecond laser.

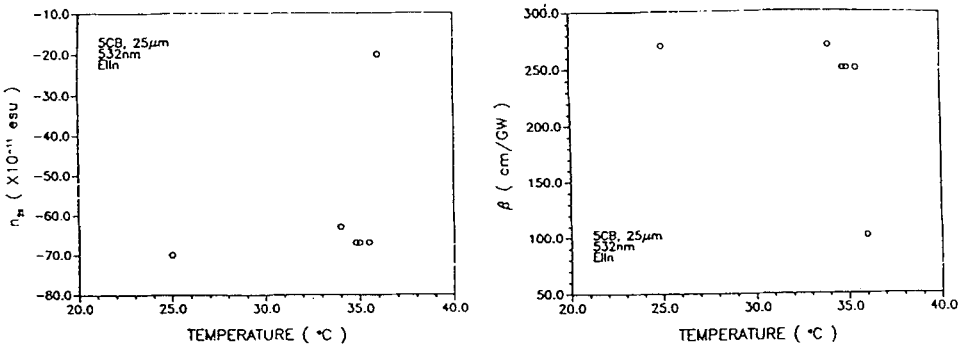

Figure 9: Temperature dependence of $n_{2||}$ and $\beta_{||}$ for a 25 μm thick 5CB.

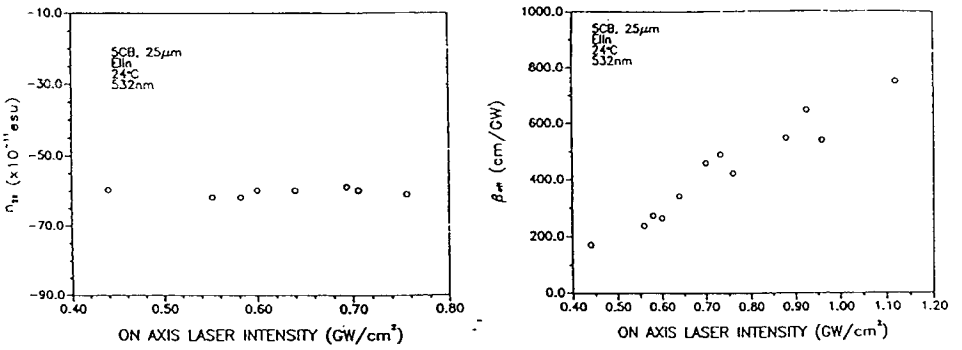

Figure 10: Intensity dependence of $n_{2\|}$ and $\beta_{\|}$ for 5CB.

sample to the second pulse differs from that of the first, then the process is slower than the pulse separation time. Using this technique, we have determined that the nonlinear refractive index change is caused by a process whose characteristic time is slower than the pulse duration, i.e., n_2 is fluence dependent. On the other hand, the nonlinear absorption process occurs on a shorter time scale, indicating that the response is only intensity dependent. These results indicates that the nonlinear absorption and refraction originate in different processes.

To further understand the underlying physical processes on nanosecond timescales, we have measured n_2 and β at different intensities. The nonlinear refractive index n_2 is constant, indicating a third order process, but the nonlinear absorption coefficient β increases with intensity, indicating a fifth order process. This is also consistent with the different response times obtained with the two-pulse Z-scan measurements.

Next, we consider the origin of the nonlinear absorption in the nanosecond regime. We note first that the process is primarily a fifth order process, i.e., the nonlinear absorption coefficient increases linearly with the incident intensity. Second, the response time of the process is shorter than 10 ns. Since β is small for picosecond pulses, this indicates that the process has time response mucher longer than 30 ps, suggesting excited state absorption. On the other hand, the linear absorption of 5CB is very small, and so the excited states cannot be due to linear absorption. The most likely process to give rise to the excited the excited states will be a two-photon process. Therefore, the nonlinear absorption process must be related to the two-photon excited state absorption.[8] Our recent experiments using a

pump-probe method indicate that there is a two-photon absorption followed by an excited state absorption. Similar conclusions have been recently reached by others.[9]

On the picosecond time scale, the $n_{2\|}$ and $n_{2\perp}$ are positive and small compared to the nanosecond results. Values for 5CB are shown below:

τ_L	λ	$n_{2\|}$ (esu)	$n_{2\perp}$	$\beta_\|$ (cm/GW)	$\beta_\perp$ (cm/GW)
33 ps	532 nm	$+13.6 \times 10^{-12}$	$+6 \times 10^{-12}$	2.27	0.8
33 ps	600 nm	$+19 \times 10^{-12}$	NA	2.67	NA
33 ps	1.06 μm	$+5.5 \times 10^{-12}$	$+5.5 \times 10^{-12}$	0	0

The nonlinear refraction here originates likely from the electronic nonlinearity, i.e., the hyperpolarizibility of the liquid crystal molecules. The nonlinear absorption is mainly from the two-photon absorption, since the band edge of linear absorption is at $\sim$ 400 nm. This explains the small nonlinear absorption at 1.06 μm.

In summary, we have extended the Z-scan technique to allow the use top-hat beams for measuring $\chi^{(3)}$. Compared with the conventional Z-scan technique, this modified scheme put less restrictions on the spatial profile of the beams which can be used for the measurement. We have also studied the mechanisms of nonlinearities on various time scales. For the nonlinear refraction on ms and ns time scales, laser heating a causes the decrease in the order parameter and density which affect the refractive indices. As a result, n_2 decreases with wavelength. On the millisecond time scale, no nonlinear absorption is observed. On the nanosecond timescale, a strong fifth order process occurs. We believe that the underlying process is a two-photon excited state absorption. On the picosecond time scale, the nonlinearity is due to hyperpolarizability and two-photon absorption. More wavelength dependent measurements are needed in order to further verify these conclusions.

This work was supported by NSF under ALCOM grant DMR89-20147 and DARPA grant DAAB07-88-F421.

REFERENCES

1. M. Sheik-Bahae, A.A. Said and E. W. Van Stryland, *Opt. Lett. 14*, 955, 1989.

2. M. Sheik-Bahae, A.A. Said, T.H. Wei, D.J. Hagan and E.W. Van Stryland, *IEEE J. Quantum Electron.* **QE-26**, 760, 1990.

3. H.J. Yuan, L. Li and P. Palffy-Muhoray, *Mol. Cryst. Liq. Cryst.* **199**, 223, 1991.

4. M. Born and E. Wolf, *Principles of Optics*, 6th ed. (Pergamon, Oxford, 1980), Sect. 8.8.

5. W. Zhao and P. Palffy-Muhoray, *Appl. Phys. Lett.* **63**, 1613, 1993.

6. L. Li, H.J. Yuan, G. Hu and P. Palffy-Muhoray, *Liq. Cryst.* (in press).

7. C.W. Greeff, *Mol. Cryst. Liq. Cryst.* **238**, 179, 1994. See also, C.W. Greeff, J. Lu and M.A. Lee, *Liq. Crsyt.* **15**, 75, 1993.

8. L. Li, G. Hu, P. Palffy-Muhoray, M.A. Lee and H.J.Yuan, *SPIE Proc.* **1692**, 107, 1992.

9. H.J. Eichler, R. MacDonald and B. Trosken, *Mol. Cryst. Liq. Cryst.* **231**, 1, 1993.